36, 2301 (1962).
[9]A. J. Freeman and R. E. Watson, Phys. Rev. 127, 2058 (1962).
[10]C. A. Hutchison Jr. and G. A. Pearson, J. Chem Phys. 47, 520 (1967).
[11]C. A. Hutchison Jr. and B. W. Mangum, J. Chem Phys. 34, 908 (1961).
[12]B. Bleaney, Phil. Mag. 42, 441 (1951).
[13]D. J. I. Fry and P. M. Llewellyn, Proc. Roy. Soc. (London) A266, 84 (1962).
[14]D. Body, K. Roberts, and A. Peterson (private communication); a variable metric method for minimization [W. C. Davidson(unpublished)], which has been developed as a computer program for previous work in this laboratory (D. Halford, Ref. 2), forms the basis for this fitting procedure.
[15]R. J. Elliott and K. W. H. Stevens, Proc. Roy. Soc. (London) A218, 553 (1953); A219, 387 (1953).
[16]J. M. Baker and B. Bleaney, Proc. Roy. Soc. (London) A245, 156 (1958).
[17]A. Abragam and B. Bleaney, *Electron Paramagnetic Resonance of Transition Ions* (Clarendon, Oxford, 1970).
[18]G. K. Woodgate, Proc. Roy. Soc. (London) A293, 117 (1966).
[19]A. J. Freeman and R. E. Watson, Phys. Rev. 132, 706 (1963).
[20]A. J. Freeman and R. E. Watson, Phys. Rev. 127, 2058 (1962).
[21]J. Blok and D. A. Shirley, Phys. Rev. 143, 278 (1966).
[22]R. M. Sternheimer, Phys. Rev. 80, 102 (1950).
[23]D. T. Edmonds, Phys. Rev. Letters 10, 129 (1963).
[24]B. R. Judd and I. Lindgren, Phys. Rev. 122, 1802 (1961).
[25]M. N. Ghatikar, A. K. Raychaudhuri, and D. K. Ray, Proc. Phys. Soc. (London) 86, 1239 (1965).
[26]R. M. Sternheimer, Phys. Rev. 132, 1637 (1963).
[27]R. E. Watson and A. J. Freeman, Phys. Rev. 135, A1209 (1964).
[28]R. M. Sternheimer, Bull. Am. Phys. Soc. 10, 597 (1965).
[29]C. J. Lenander and E. Y. Wong, J. Chem. Phys. 38, 2750 (1963).
[30]D. K. Ray, Proc. Phys. Soc. (London) 82, 47 (1963).

PHYSICAL REVIEW B VOLUME 5, NUMBER 9 1 MAY 1972

Nuclear Magnetic Resonance and Nuclear-Spin Dynamics in InP†

M. Engelsberg* and R. E. Norberg
Department of Physics, Washington University, St. Louis, Missouri 63130
(Received 13 August 1971)

Pulsed- and steady-state nuclear-magnetic-resonance measurements are reported for P^{31} in InP. Measurements on "solid echoes" permit identification of various contributions to the second moment of the resonance. The dominant P^{31}–$In^{115,113}$ contribution is found to be about a factor of 2 smaller than expected from dipole-dipole interactions alone. A proposed explanation is based on interference between pseudodipolar and dipolar interactions of similar magnitude but opposite sign. The time evolution of the P^{31} magnetization along the effective field in the rotating frame indicates the presence of a significant cross-relaxation effect involving the resonant spin-Zeeman reservoir and the nonresonant spin-spin reservoir.

I. INTRODUCTION

The extensive studies of III-V compounds in recent years have included a variety of nuclear-magnetic-resonance (NMR) experiments[1] in which special attention was given to the electron-coupled nuclear-spin interactions.[2–4] The linewidths of the III-V compounds containing the heavier elements have been explained on the basis of the indirect-exchange interaction between unlike nuclear spins,[5–8] which has a broadening effect on the NMR line of either spin. However, the role of the pseudodipolar interaction[3] in some of these compounds is not clear. The electronic valence band is predominantly p-like and a large density of p states in the conduction band away from the center of the Brillouin zone may be a characteristic shared by all III-V compounds containing phosphorus.[9] InP appears to be an appropriate system to search for electron-coupled interactions. P^{31} is 100% abundant and is the only nuclear species within this group of compound with spin $I=\frac{1}{2}$. Thus the second moment of the InP^{31} resonance is not affected by quadrupole effects. In addition, because of the large atomic number of indium, P^{31}–$In^{115,113}$ electron-coupled interactions are expected to play a more important role in InP than in the other phosphides. Moreover, since P^{31}–P^{31} dipole-dipole interactions are small compared to P^{31}–$In^{115,113}$ interactions, any departure of the latter from the purely dipolar value has an appreciable effect on the P^{31} linewidth.

There are three magnetic ingredients in InP: P^{31}, In^{115}, and In^{113}. The two indium isotopes have spins $S=\frac{9}{2}$, similar gyromagnetic ratios, and similar quadrupole moments. In addition, In^{113} is only 4.16% abundant. Thus the difference between the

two indium isotopes does not have an appreciable effect on the P^{31} resonance, and for most purposes one can assume that In^{115} is 100% abundant.

An interesting aspect of this system of spins results from the study of the dynamics of the $P^{31}-In^{115}$ energy-transfer process in the rotating frame. The nature of the cross-relaxation effect in InP permits investigation of the mechanism leading to a uniform spin temperature[10–12] in the rotating frame and confirmation of the validity of simple thermodynamical arguments[13] in connection with rotating frame cross relaxation between dissimilar spins.[14]

II. NMR IN InP

A. Experimental Details

Pulsed NMR experiments on InP^{31} were performed at 15 and 30 Mcps. No field dependence of the P^{31} free-induction-decay (FID) signal was observed and most of the data were taken at 15 Mcps with a pulsed spectrometer based on an NMR Specialties PS60 pulse system. A single receiver and transmitter coil was employed to produce a linearly polarized rf field of a maximum amplitude of about 90 G corresponding to a 90° nutation of the P^{31} magnetization in about 3.3 μsec. Pulsed experiments in InP^{31} were performed at three fixed temperatures: 300, 78, and 4.2 °K.

Steady-state measurements on InP^{31} were performed at room temperature at a frequency of 11.23 Mcps using a conventional Pound-Knight-Watkins[15] spectrometer. The static magnetic field was modulated with a 100-cps sine-wave modulation of small amplitude compared to the expected resonance linewidth and swept through resonance at a rate of 1 G/min.

The InP samples studied were various n-type and p-type materials. The powdered samples had an average particle size of 0.05 mm and sample 5^c was a single crystal. The n-type materials were undoped whereas the p-type samples were doped with zinc or cadmium. The measured P^{31} spin-lattice relaxation times in our samples ranged from 1700 sec for samples 5 and 5^c to about 10 sec for sample 6 at 78 °K. All InP samples were made available by the New Enterprise Division of the Monsanto Company, who also supplied the mobility data at room temperature. Most of the results presented here were obtained from the three materials listed in Table I which shows some relevant characteristics of the samples.

The skin depths δ at 15 Mcps were calculated from the conductivity data. For sample 5 one obtains $\delta \sim 1$ cm, which is of the order of the dimension of our single-crystal sample (sample 5^c). Effects due to nonuniform penetration of the rf field into the sample were not observed, however. In the powdered samples the calculated skin depths were much larger than the particle size and no skin effects were expected.

B. Line-Shape and Second-Moment Measurements in InP

Figure 1 shows a semilogarithmic plot of the P^{31} FID signal amplitude as a function of the square of time measured from the end of a 90° rf pulse. The experimental points are averages over six traces using sample 5 at 78 °K. In Fig. 1, a Gaussian extrapolation to $t=0$ is made. This plausible procedure can be justified in our case by the shape of the $90°\text{-}\tau\text{-}90°_{90°}$ echo signal. As will be discussed in Sec. IIC, the echo signal which approaches the FID for short τ has a Gaussian shape in the region where the FID is unobservable.

The second moment of the unsaturated resonance line is determined by the second derivative of the FID[16] $G(t)$ at $t=0$. We have

$$\langle \Delta\omega^2 \rangle = \frac{-(d^2G/dt^2)_{t=0}}{G(0)} \quad . \tag{1}$$

In our case, the extrapolated FID signal starts to deviate from a Gaussian curve only after it has decayed to about 40% of its initial value. In the region where the FID in Fig. 1 coincides with a Gaussian, the approximation

$$\begin{aligned} G(t)/G(0) &= e^{-\langle \Delta\omega^2 \rangle t^2/2} \\ &\simeq 1 - (1/2!)\langle \Delta\omega^2 \rangle t^2 + (3/4!)\langle \Delta\omega^2 \rangle^2 t^4 \\ &\quad - (15/6!)\langle \Delta\omega^2 \rangle^3 t^6 \end{aligned} \tag{2}$$

is valid to better than 1%.[17] Thus, to a very good approximation, the second moment and also the fourth moment of the resonance can be calculated from the slope of the straight line in Fig. 1. The result for the second moment is

$$(\Delta H^2)^{P31}_{FID} = \langle \Delta\omega^2 \rangle / \gamma^2_{P31} = 1.9 \pm 0.1 \text{ G}^2 \quad . \tag{3}$$

No change in the P^{31} second moment and no significant change in the FID was observed as a function of sample material or temperature.

TABLE I. Some characteristics of the InP samples.

	Samples[a] 5, 5^c	Sample 6	Sample 7
Carriers (300 °K) (cm^{-3})	$n = 2.3\times10^{15}$ to 4.2×10^{15}	$p = 2.5\times10^{18}$	$n = 2\times10^{17}$
Dopant		Zn ≃ 0.1%	
Principal impurity	Mg < 0.005%	Si < 0.05%	Mg < 0.005%
P^{31} spin-lattice relaxation time at 78 °K (sec)	1700	10	102

[a]Samples 5, 6, and 7 are powders. Sample 5^c is a single crystal.

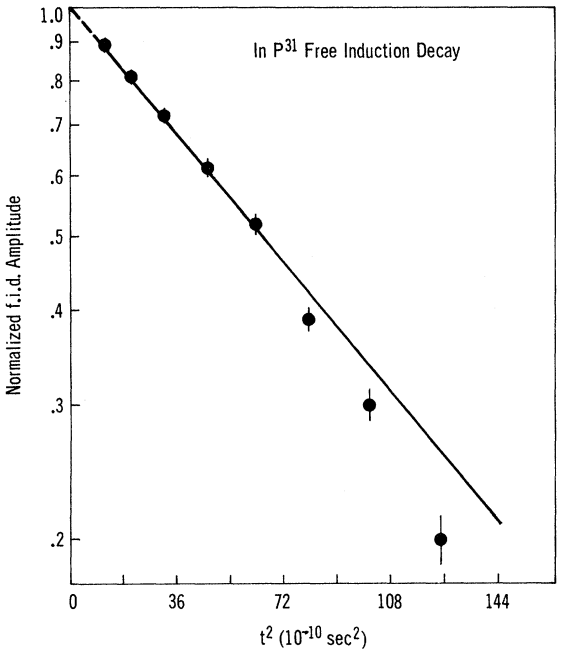

FIG. 1. InP^{31} FID amplitude as a function of t^2.

Figure 2 shows a P^{31} absorption derivative spectrum in InP. Special care was necessary to avoid saturation that could distort the P^{31} line shape. All cw measurements on InP^{31} were therefore made on sample 6 which shows the shortest spin-lattice relaxation time T_1. A plot of P^{31} signal amplitude vs rf voltage indicated that for the lowest rf level used, saturation effects were negligible. Second moments computed from the cw spectra were corrected for modulation broadening[18] which amounted to about 18% of the measured P^{31} second moment.

For long times, the FID in Fig. 1 decays faster than predicted by the initial Gaussian. Consequently, the P^{31} cw absorption signal cannot be fitted by a single Gaussian line. In addition to the P^{31} absorption derivative spectrum, Fig. 2 shows the derivative of a Gaussian function with a second moment $(\Delta H^2) = 4.24\ G^2$, which is the value expected from purely magnetic dipole-dipole interactions for a powdered sample. The distance between maxima of the absorption derivative is $\delta H = 3.6$ G (a value $\delta H = 3.8$ G was previously reported[19]). If one assumes a Gaussian line shape with $\delta H = 3.6$ G, the second moment would have a value $\frac{1}{4}\delta H^2 = 3.24\ G^2$. In fact, the correct experimental second moment, obtained by an integration[20] using both halves of the absorption derivative and averaged over four traces, is

$$(\Delta H^2)_{cw}^{P^{31}} = 2.0 \pm 0.1\ G^2 . \qquad (4)$$

The agreement with the FID result is satisfactory.

C. "Solid Echoes" in InP^{31}

Powles and Strange[17] first demonstrated how "solid echoes" could be used to achieve zero time resolution in pulsed NMR. Their result was extended to a system with two magnetic ingredients by Mansfield,[21] who also indicated the possibility of using the method to measure separately the contributions to the second moment from like and unlike spins.

In the following discussion we will assume that InP is a system composed of two magnetic ingredients (P^{31} and In^{115}) and that P^{31} is the resonant spin.

The nuclear-spin Hamiltonian, in frequency units, can be written quite generally in the high-field approximation as

$$\mathcal{H} = \mathcal{H}_0 + \mathcal{H}_1 = -\gamma_I H_0 \sum_j I_{jz} - \gamma_S H_0 \sum_{k'} S_{k'z} + \sum_{jk'} C_{jk'}^{IS} I_{jz} S_{k'z}$$

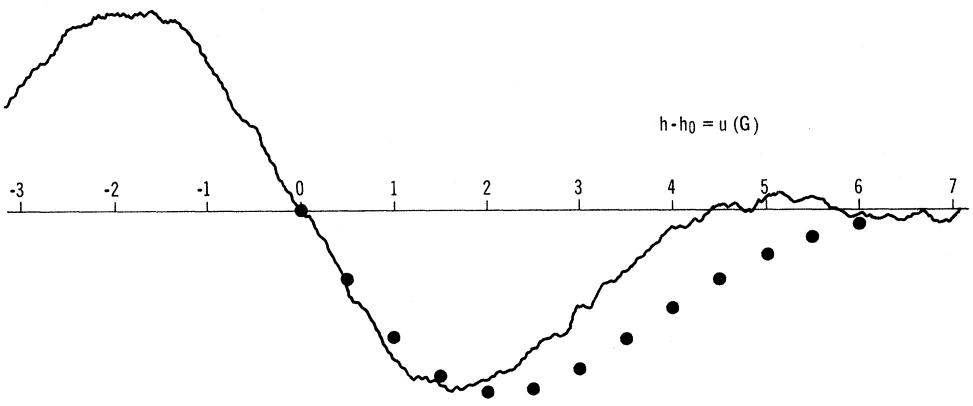

FIG. 2. Recorder trace of the derivative of the InP^{31} cw resonance absorption. The solid circles represent the derivative of a Gaussian function with a second moment equal to that expected from magnetic dipole-dipole interactions alone.

$$+\sum_{k>j}(A^I_{jk}\vec{I}_j\cdot\vec{I}_k+B^I_{jk}I_{jz}I_{kz})$$

$$+\sum_{k'>j'}(A^S_{j'k'}\vec{S}_{j'}\cdot\vec{S}_{k'}+B^S_{j'k'}S_{j'z}S_{k'z})+\mathcal{H}^S_Q\ . \quad (5)$$

The term $\mathcal{H}_1=\mathcal{H}_{II}+\mathcal{H}_{SS}+\mathcal{H}_{IS}+\mathcal{H}^S_Q$ in Eq. (5) contains dipole-dipole and electron-coupled interactions between resonant spins $\mathcal{H}_{II}$ and nonresonant spins $\mathcal{H}_{SS}$ as well as the secular part of the cross-coupling interaction $\mathcal{H}_{IS}$ and the quadrupole interactions of the nonresonant spins $\mathcal{H}^S_Q$. $\mathcal{H}_0$ is the Zeeman interaction of the resonant and nonresonant spins with the external magnetic field H_0.

The decay of the transverse magnetization following a $90°$-τ-θ_ϕ sequence (θ is the nutation angle and ϕ is the rf phase shift between the two pulses) has been calculated by Mansfield.[21] The result is

$$\frac{\langle I_x\rangle}{\langle I_x\rangle_0}=\frac{1}{\mathrm{Tr}(I_x^2)}\,\mathrm{Tr}\Big(I_x^2+i^2[\mathcal{H}_1',[\mathcal{H}_1',I_x]]I_x\frac{\tau^2}{2!}$$
$$-[\mathcal{H}_1',I_x][\mathcal{H}_1,I_x]t'\tau+[\mathcal{H}_1,[\mathcal{H}_1,I_x]]I_x\frac{t'^2}{2!}$$
$$+\text{terms of order }(t^n\tau^m)\Big)\ (\text{with } n+m\geq 4)\ , \quad (6)$$

where $\mathcal{H}_1'=R^\dagger_{(2)}\mathcal{H}_1R_{(2)}$ and $R_{(2)}$ is the rotation operator corresponding to the second pulse. That is, $R_{(2)}=e^{i\theta I_x}$ or $R_{(2)}=e^{i\theta I_y}$ for $\phi=90°$ or $\phi=0°$, respectively. The second pulse is applied at time τ after the first pulse and t' is the time measured from the second pulse.

One can see from Eq. (6), using the identity $\mathrm{Tr}\{[A,[A,I_x]]I_x\}=-\mathrm{Tr}[A,I_x]^2$, that to second order in time the echo signal is not affected by the terms $\mathcal{H}_{SS}+\mathcal{H}^S_Q$ in Eq. (5) involving only nonresonant spins.

1. $90°$-τ-$90°_{90°}$ *Sequence*

For $\tau>40$ μsec the InP^{31} echo signal shows a well-resolved maximum at $t'=\tau$. The echo shape does not deviate appreciably from the FID for short τ and only changes slowly for larger values of τ. The echo amplitude $\langle I_x\rangle_\tau$, however, is a rapidly decreasing function of τ.

Defining the quantity $R(t'\tau)=\langle I_x\rangle/\langle I_x\rangle_0$, where $\langle I_x\rangle_0$ is the amplitude of the FID, one obtains for sufficiently small τ[21]

$$R''(\tau)=-\left(\frac{d^2R(t'\tau)}{dt'^2}\right)_{t'=\tau}$$
$$=[(\Delta\omega^2_{II})+(\Delta\omega^2_{IS})]-\Delta_{4\epsilon}\tau^2\ . \quad (7)$$

Here $(\Delta\omega^2)=(\Delta\omega^2_{II})+(\Delta\omega^2_{IS})$ is the total second moment of the resonant spin and $\Delta_{4\epsilon}$ is a fourth-moment-type correction term. Figure 3 shows a plot of $R''(\tau)$ as a function of τ^2. The data were obtained from sample 6 at 78 °K. Most of the variation of $R''(\tau)$ comes from the normalizing factor $R(\tau)=\langle I_x\rangle_\tau/\langle I_x\rangle_0$ which is contained in $R''(\tau)$. The intercept of the straight line corresponds to

$$(\Delta H^2)^{P^{31}}_{\text{echo}}=2.15\pm0.15\ \text{G}^2\ , \quad (8)$$

in reasonable agreement with $(\Delta H^2)^{P^{31}}_{cw}$ and $(\Delta H^2)^{P^{31}}_{FID}$.

The $90°$-τ-$90°_{90°}$ echo amplitude $\langle I_x\rangle_\tau$ is expected to decay as[21]

$$R(\tau)=\langle I_x\rangle_\tau/\langle I_x\rangle_0\simeq 1-(\Delta\omega^2_{IS})\tau^2 \quad (9)$$

for sufficiently small τ. From the predicted τ^2 dependence, valid for $\tau\lesssim 40$ μsec, one obtains

$$(\Delta H^2_{IS})^{P^{31}}_{\text{echo}}=2.1\pm0.2\ \text{G}^2. \quad (10)$$

Since the contribution to the second moment from like spins $(\Delta H^2_{II})^{P^{31}}$ seems to be the same order of magnitude as the experimental error involved in the measurement of $(\Delta H^2_{IS})^{P^{31}}$ or $(\Delta H^2)^{P^{31}}$, its magnitude can only be determined by direct measurement.

2. $90°$-τ-$180°$ *Sequence*

This case was not explicitly treated by Mansfield.[21] Since the sequence allows an independent measurement of $(\Delta H^2_{II})^{P^{31}}$, it deserves some attention. No echo signal is expected from a $90°$-τ-$180°$ pulse sequence for a system with only one magnetic ingredient in a homogeneous magnetic field. The term $\mathcal{H}_{II}$ in Eq. (5), being a quadratic function of the spin operators, is not changed by the transformations $\mathcal{H}_I'=R^\dagger_{(2)}\mathcal{H}_IR_{(2)}$ where $R_2=e^{i\pi I_x}$ is the rotation operator corresponding to a $180°$ pulse. As a consequence the $180°$ pulse has no effect and no echo is observed for a single-spin species.

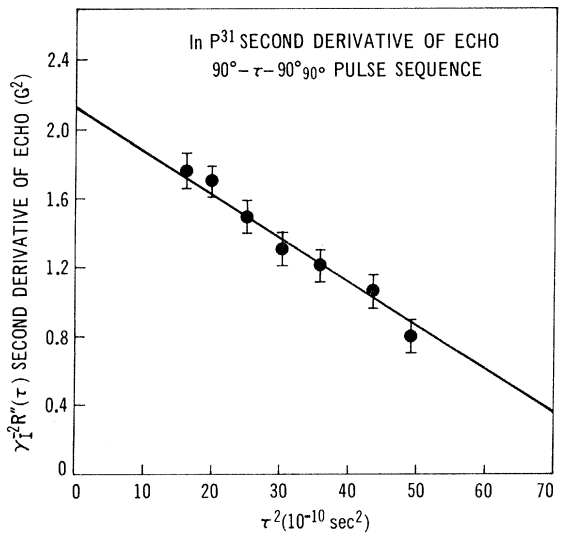

FIG. 3. Second derivative of the normalized P^{31} echo signal at $t'=\tau$ as a function of the square of the pulse separation for a $90°$-τ-$90°_{90°}$ pulse sequence. The normalization factor is the inverse of the FID signal amplitude immediately following the first $90°$ pulse.

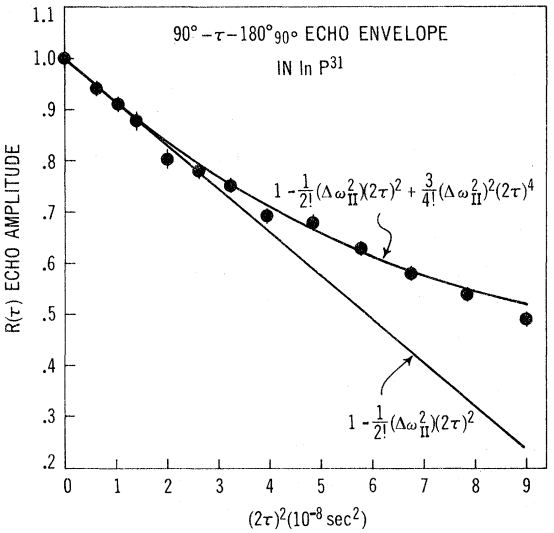

FIG. 4. P^{31} echo envelope for a $90°-\tau-180°_{90°}$ pulse sequence as a function of $(2\tau)^2$.

In our case, however, we have

$$\mathcal{H}_1' = R_{(2)}^{\dagger}\mathcal{H}_1 R_{(2)} = \mathcal{H}_{II} + \mathcal{H}_{SS} + \mathcal{H}_Q^S - \mathcal{H}_{IS} \ . \qquad (11)$$

The presence of the term

$$\mathcal{H}_{IS} = \sum_{jk'} C_{jk'}^{IS} I_{jz} S_{k'z}$$

gives rise to a well-defined echo after a $90°-\tau-180°$ pulse sequence.[22,23]

The echo envelope $R(\tau)$ as a function of pulse separation τ can be calculated from Eq. (6) to second order in τ. With $\mathcal{H}_1'$ given by Eq. (11) one obtains after little algebra

$$R(\tau) = 1 - (\Delta\omega_{II}^2)\frac{(2\tau)^2}{2!} + \epsilon_4 \frac{(2\tau)^4}{4!} + \cdots \ . \qquad (12)$$

Thus, for sufficiently small τ, a τ^2 dependence is expected.

Figure 4 shows a plot of experimental values $R(\tau)$ as a function of $(2\tau)^2$. Also shown are the second- and fourth-order approximations to $R(\tau)$ indicated in Eq. (12). For the fourth-order approximation a value $\epsilon_4 = 3(\Delta\omega_{II}^2)^2$ fits the experimental data reasonably well. From Fig. 4 one obtains

$$(\Delta H_{II}^2)_{\text{echo}}^{P^{31}} = 0.15 \pm 0.01 \ \text{G}^2 \ . \qquad (13)$$

The theoretical value obtained assuming only magnetic dipole-dipole interactions is $(\Delta H_{II}^2)_{\text{dipolar}}^{P^{31}} = 0.165 \ \text{G}^2$.

Table II contains a summary of the various experimental second moments and also shows the calculated values for a powdered sample assuming purely magnetic dipole-dipole interactions.[24] The lattice sums involved in the calculation of the second moments were evaluated by adding the contributions of 16 shells of atoms. Contributions from more remote atoms were taken into account through an integration over a uniform distribution. The calculated dipolar moments agree with previous calculations.[25] The value of the lattice constant[26] for InP is $a = 5.86875$ Å at 20 °C.

D. Discussion of Experimental Results and Conclusions

The data summarized in Table II contain a rather remarkable result. The experimental second moment of the P^{31} resonance is about a factor of 2 smaller than the calculated $(\Delta H^2)_{\text{dipolar}}^{P^{31}}$. An interaction between unlike spins seems to be responsible for the effect. The contribution to the second moment from like spins agrees with the calculated $(\Delta H_{II}^2)_{\text{dipolar}}^{P^{31}}$.

The second moment of a resonance line may be difficult to measure in some cases where "narrowing effects" strongly affect the line shape. The presence in the interaction Hamiltonian of terms commuting with I_x has no effect on the second moment of the resonance of the spin I but may considerably increase its fourth moment. As a result, the wings of the resonance can be enhanced and the center narrowed, resulting in a line shape approaching a Lorentzian.

In InP "narrowing effects" do not appear to affect the P^{31} resonance line. Motional narrowing can certainly be ruled out at room temperature and below.[27] An exchange interaction between P^{31} spins, large enough to produce a narrowing effect in InP^{31}, would be difficult to justify. In addition, the $90°-\tau-180°_{90°}$ echo envelope does not show any indication of such an effect in InP^{31}.

The effect on the P^{31} line shape of the terms $\mathcal{H}_{SS} + \mathcal{H}_Q^S$, where S refers to the nonresonant indium spins, must also be considered. Previous investigations[8,28] seem to indicate that for our undoped samples, second-order quadrupole effects may be negligible. One can therefore write[8] $\mathcal{H}_Q = \sum_j E_j[3S_{zj}^2 - S(S+1)]$. Since the III-V compounds have the zinc-blende crystal structure, the electric field gradients that determine the quadrupole coupling constant E_j are produced by impurities and lattice imperfections.[28] The fourth moment[24] of the resonance of the spin I is proportional to $\text{Tr}\{[\mathcal{H}_1[\mathcal{H}_1, I_x]]\}^2$,

TABLE II. Second moments of the InP^{31} NMR.

Calculated (G^2)	Measured (G^2)
$(\Delta H_{II}^2)_{\text{dipolar}}^{P^{31}} = 0.165$	$(\Delta H_{II}^2)_{\text{echo}}^{P^{31}} = 0.15 \pm 0.01$
$(\Delta H_{IS}^2)_{\text{dipolar}}^{P^{31}} = 4.076$	$(\Delta H_{IS}^2)_{\text{echo}}^{P^{31}} = 2.10 \pm 0.2$
	$(\Delta H^2)_{\text{FID}}^{P^{31}} = 1.9 \pm 0.1$
$(\Delta H^2)_{\text{dipolar}}^{P^{31}} = 4.241$	$(\Delta H^2)_{\text{cw}}^{P^{31}} = 2.0 \pm 0.1$
	$(\Delta H^2)_{\text{echo}}^{P^{31}} = 2.15 \pm 0.15$

where $\mathcal{H}_1$ is given by Eq. (5). Since $\mathcal{H}_Q^S$ commutes with $[\mathcal{H}_1, I_x]$, its contribution to the fourth moment vanishes. Thus $\mathcal{H}_Q^S$ would affect the InP^{31} FID only for relatively long times. In fact, no significant variation of the FID was observed as a function of sample material.

The spin-spin interaction between indium spins, represented by $\mathcal{H}_{SS}$ in Eq. (5), contains the term

$$\tfrac{1}{2}\sum_{k'>j'} A^S_{j'k'}(S_{j'+}S_{k'-}+S_{j'-}S_{k'+}) ,$$

which does not commute with $\mathcal{H}_{IS}$ and therefore contributes to the fourth moment of the P^{31} resonance. If $A^S_{j'k'}$ were much larger than $C^{IS}_{jk'}$, a line shape approaching a Lorentzian could result.[29] In the present case, however, $A^S_{j'k'}$ would be smaller than $C^{IS}_{jk'}$ if only dipole-dipole interactions were present. An isotropic exchange interaction between indium spins might increase $A^S_{j'k'}$ by a factor[8] of the order of 2 above the dipolar value. Since the gyromagnetic ratio of indium is about a factor of 2 smaller than that of phosphorus, the term

$$\tfrac{1}{2}\sum_{k'>j'} A^S_{j'k'}(S_{j'+}S_{k'-}+S_{j'-}S_{k'+})$$

is not expected to produce a narrowing effect on the P^{31} resonance line. Instead of approaching a Lorentzian, the wings go to zero faster than the initial Gaussian (Fig. 2).

We postulate that the coefficient $C^{IS}_{jk'}$ in Eq. (5) can be written as

$$C^{IS}_{jk'} = \tilde{A}^{IS}_{jk'} + (\gamma_I\gamma_S\hbar/r^3_{jk'} + \tilde{B}^{IS}_{jk'})(1-3\cos^2\theta_{jk'}) , \tag{14}$$

where the magnetic dipole-dipole and electron-coupled interactions[3] are included. The coefficients $\tilde{A}^{IS}_{jk'}$ and $\tilde{B}^{IS}_{jk'}$ represent exchange and pseudodipolar interactions between unlike spins.

The contribution to the second moment of the resonant spins I (in our case P^{31}) from interactions with the nonresonant spins S[24] can be calculated from Eq. (14). For a powdered sample one obtains

$$(\Delta\omega^2_{IS})^I = (\Delta\omega^2_{IS})^I_{\text{dipolar}} + \tfrac{1}{3}S(S+1)\sum_{k'}(\tilde{A}^{IS}_{jk'})^2 + \tfrac{4}{15}S(S+1)\sum_{k'}\left((\tilde{B}^{IS}_{jk'})^2 + \frac{2\gamma_I\gamma_S\hbar\tilde{B}^{IS}_{jk'}}{r^3_{jk'}}\right) . \tag{15}$$

For negative values of $\tilde{B}^{IS}_{jk'}$, the last term in Eq. (15) can cause a reduction of $(\Delta\omega^2_{IS})^I$ from its purely dipolar value.

Substituting in (15) the calculated $(\Delta\omega^2_{IS})^{P^{31}}_{\text{dipolar}}$ and the experimental quantity $(\Delta\omega^2_{IS})^{P^{31}}$, a quadratic equation is obtained, which has real solutions $\tilde{B}^{IS}$ provided that

$$|\tilde{A}^{IS}| \leq 2.2\times10^3 \text{ sec}^{-1} . \tag{16}$$

The roots of Eq. (15) corresponding to values $\tilde{A}^{IS}$ in a range Eq. (16) would then satisfy

$$-6.4\times10^3 \text{ sec}^{-1} \leq \tilde{B}^{IS} \leq -1.6\times10^3 \text{ sec}^{-1} , \tag{17}$$

where $\tilde{A}^{IS}$ and $\tilde{B}^{IS}$ represent electron-coupled interactions between nearest neighbors, and contributions to the lattice sums [Eq. (15)] from more remote neighbors have been neglected. There is no ambiguity in the sign of $\tilde{B}^{IS}$, which is opposite to that of the magnetic dipole-dipole interaction.[30]

The experimental results in our powdered samples allow us to obtain a lower limit for the ratio $|\tilde{B}^{IS}/\tilde{A}^{IS}|$. From Eq. (15) the value of $|\tilde{A}^{IS}|$ that minimizes the ratio $|\tilde{B}^{IS}/\tilde{A}^{IS}_m|$ is $|\tilde{A}^{IS}_m| = 1.7\times10^3 \text{ sec}^{-1}$ and the corresponding value $|\tilde{B}^{IS}_m| = 2.5\times10^3 \text{ sec}^{-1}$. The experimental results on our powdered samples would then also imply $|\tilde{B}^{IS}/\tilde{A}^{IS}| \geq 1.5$.

For a single crystal of InP, a considerable anisotropy of the second moment of the P^{31} resonance would be expected on the basis of magnetic dipole-dipole interactions alone. When the magnetic field is along a [100] direction, the dipole-dipole interactions between unlike nearest neighbors vanishes in a zinc-blende structure. Thus, if the magnetic field is rotated in some plane containing a [100] axis, the expected anisotropy would be large.

Single-crystal measurements were performed on sample 5^c. The crystal was rotated about an axis in the [100] plane making an angle of about 45° with the [001] direction and with the external magnetic field perpendicular to the rotation axis. For this particular geometry a variation of the second moment by a factor of about 2.5 would be expected from dipole-dipole interactions alone. In fact, no change in the second moment of the FID was observed as a function of crystal orientation. The measured value coincided, within the experimental error, with the result obtained for our powdered samples.

The lack of anisotropy may be interpreted to indicate that the pseudodipolar interaction and the magnetic dipole interaction are of the same order of magnitude and largely cancel each other. From Eq. (14) one would obtain

$$\tilde{B}^{IS} \simeq -\gamma_I\gamma_S\hbar/r^3 = -4\times10^3 \text{ sec}^{-1} . \tag{18}$$

The corresponding value of $|\tilde{A}^{IS}|$ can then be calculated from Eq. (15). The result is

$$|\tilde{A}^{IS}| \simeq 2.2\times10^3 \text{ sec}^{-1} . \tag{19}$$

A ratio $|\tilde{B}^{IS}/\tilde{A}^{IS}| \simeq 1.8$ would then result from our single-crystal experimental data.

Relatively little data on the magnitude of the pseudodipolar interaction in nonmetallic solids have been reported so far.[3,31,32] Bloembergen and Sorokin[31] determined the magnitude of the Cs-Br electron-coupled interactions in CsBr. Although the sign of $\tilde{B}^{IS}$ could not be uniquely determined from their experiments, one of the two possible

results was a negative one with a ratio $|\tilde{B}^{IS}/\tilde{A}^{IS}| = 1.6$. A negative value for the pseudodipolar interaction between Tl^{205} spins in TlCl was also reported by Clough and Goldburg.[32]

Some understanding of the nature of the electron-coupled interactions in solids with a partially covalent bond can be obtained from a simple localized bond model.[31-33] The ratio $|\tilde{B}^{IS}/\tilde{A}^{IS}|$ in this model is independent of the degree of covalency of the bond; it depends on the amounts of s and p character of the electronic wave functions, and it vanishes for purely s-like states.[32] Since the hyperfine interaction with s electrons is larger than with p electrons, a ratio $|\tilde{B}^{IS}/\tilde{A}^{IS}| \simeq 1$ implies a predominantly p character of the electronic wave function. An interesting consequence of this model is that it predicts a negative value[31,32] of $\tilde{B}^{IS}$ in agreement with our experimental result in InP.

A more realistic approach to the present problem would be to describe the electronic states by Bloch-type wave functions. Previous calculations of electron-coupled interactions in the III-V compounds[4,5] did not take into account hyperfine interactions with p electrons. Although a more refined calculation that removes this restriction will not be attempted here, some qualitative arguments will be presented.

Our experimental results seem to indicate a significantly larger ratio $|\tilde{B}^{IS}/\tilde{A}^{IS}|$ in InP than in InSb.[5,8] The contribution to the nuclear-spin Hamiltonian from electron-coupled interactions is given by[3]

$$\tilde{\mathcal{H}}_{IS} = \sum_{kk'} \sum_{ss'} |(\psi_{k's'}|\mathcal{H}_{en}|\psi_{ks})|^2 [E(\vec{k}) - E(\vec{k}')]^{-1} , \tag{20}$$

where $\mathcal{H}_{en}$ includes the contact and dipolar hyperfine interactions with a pair of nuclear spins, and only terms bilinear in both nuclear spins are retained in Eq. (20). The summation extends over all initially occupied states $\vec{k}$, $\vec{s}$ and all excited states $\vec{k}'$, $\vec{s}'$.

The integral involved in Eq. (20) contains the factor $\Delta_{kk'} = g_v(\vec{k}) \times g_c(\vec{k}') [E(\vec{k}) - E(\vec{k}')]^{-1}$, where $g_v(\vec{k})$ and $g_c(\vec{k}')$ are densities of states in the valence bands and conduction bands, respectively, and $[E(\vec{k}) - E(\vec{k}')]$ is the corresponding energy difference.

The density of states in the conduction bands[34] of InP, away from the center of the zone, can be as much as 50 times larger than the density of states of the lowest-energy conduction band at $k = 0$.[35] Despite the larger energy denominator, these states could make a dominant contribution to $\Delta_{kk'}$. Moreover, because of the proximity of the second lowest conduction band, predominantly p-like, to the first conduction band along directions like [100],[34] these states could contribute to the pseudodipolar interaction. The position of the p-like bands is rather insensitive to the atomic number of the atoms involved.[35] In InSb, however, the first conduction band, predominantly s-like, is much closer to the valence band. A smaller ratio $|\tilde{B}^{IS}/\tilde{A}^{IS}|$ than in InP would then be expected.

III. NUCLEAR-SPIN DYNAMICS IN InP

A. Rotating Frame Experiments and Thermodynamical Model

Spin-locking[36] experiments were performed in InP^{31} to study the time evolution of the P^{31} magnetization along the effective field in the rotating frame. In addition, the response to a train of 90° pulses in a sequence[37,38] $90°\text{-}\tau\text{-}90°_{90°}\text{-}2\tau\text{-}90°_{90°}\text{-}2\tau\cdots$ was studied as a function of pulse separation 2τ.

The envelope of the train of "solid echoes" shows some distinctive features. As observed in a similar experiment[39] on $Na^{23}F$, there is a sharp initial drop of signal amplitude during the first echo. This is implicit in Eq. (9). The echo envelope oscillates with a period[38] 8τ for a time of about 500 μsec [Fig. 5(a)] and then decays monotonically. Unlike the $Na^{23}F$ case, however, the InP^{31} chain does not settle down to a single exponential decay. The fast initial decay, characterized by a time constant T_{IS}, is followed by a much slower one [Fig. 5(b)].

Except for the slow final decay which is slower in the spin-locking experiment, the time evolution of the "spin-locked" magnetization agrees reasonably well with the decay of the echo envelope for an effective field $H_1 = \pi/4\gamma_I\tau$.

For the values of rotating field H_1 involved in our experiments, spin-lattice processes do not significantly affect the decay of the magnetization along the effective field in the rotating frame. A dependence of the time constant T_{IS} on sample material was observed, but the samples with shorter P^{31} spin-lattice relaxation times exhibited longer values of T_{IS}. The observed temperature independence of T_{IS} seems to indicate that In^{115} spin-lattice relaxation[40] also has a negligible effect on the decay.

In the spin-locking experiment a rf field, at the resonant frequency of the I spins (in our case P^{31}) and perpendicular to the external field H_0, is applied to the system. The Hamiltonian will contain, in addition to the terms included in Eq. (5), the coupling energy of the I and S spins with the rf field.

The effect of strong rf irradiation by a rotating field H_1 is better understood if the density matrix of the system of spins is transformed to a rotating frame[10] by the transformation

$$\exp[-i\gamma_I H_0(I_z + S_z)t]\,\rho(t)\exp[i\gamma_I H_0(I_z + S_z)t] .$$

Since the condition $|1 - (\gamma_I/\gamma_S)|H_0 \gg H_1$ is well satisfied in InP, the contribution to the effective Hamiltonian in the rotating frame from the coupling of the nonresonant spins S with the rotating field H_1 can be neglected.[10] The effective Hamiltonian relevant to our problem is given by

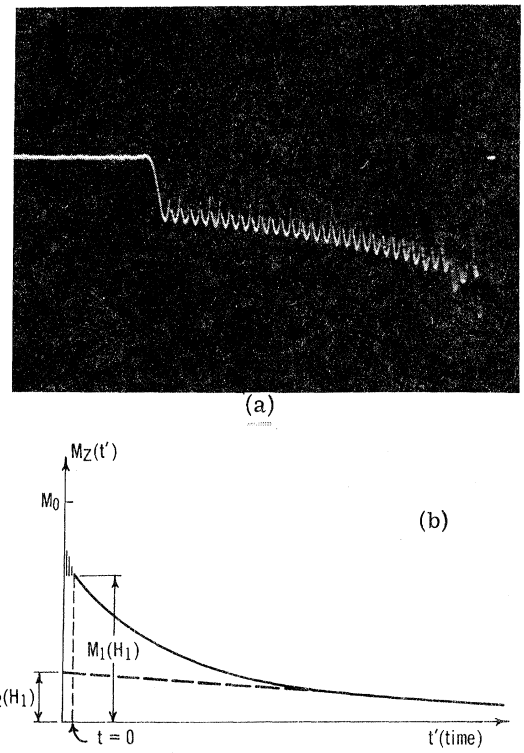

FIG. 5. (a) Oscilloscope photograph of a train of "solid echoes" for a $90°$-τ-$90°_{90°}$-2τ-$90°_{90°}$-2τ-$90°_{90°}$-$\cdots$ pulse sequence in InP^{31}. The pulse separation is $2\tau = 100$ μsec and the sweep is 0.5 msec/large div. (b) Sketch of the echo envelope showing the fast initial decay and the slower final decay. The total time is typically 20 times longer than in (a).

$$\mathcal{H}_{e\rho} = -\gamma_I H_1 I_Z + \sum_{k>j} (A^I_{jk} \vec{I}_j \cdot \vec{I}_k + B^I_{jk} I_{jX} I_{kX}) + \sum_{jk'} C^{IS}_{jk'} I_{jX} S_{k'z} + \mathcal{H}_S \,, \qquad (21)$$

where the Z axis is along the rotating field and the transformation $I_x = I_Z$, $I_y = I_Y$, $I_z = -I_X$ has been used. $\mathcal{H}_S = \mathcal{H}_{SS} + \mathcal{H}^S_Q$ is given by Eq. (5).

In the multiple-pulse experiments, the amplitude of the rf field is modulated by pulses. One can expand the modulation signal in a Fourier series.[38] For a $90°$-τ-$90°_{90°}$-2τ-$90°_{90°}$-$2\tau\cdots$ pulse sequence at the resonant frequency of the I spins, the contribution from the zeroth-order term in the Fourier expansion is a rotating field of amplitude $H_1 = \pi/4\gamma_I\tau$ at exact resonance. The effect of the higher harmonics of the modulation frequency[38] $\omega_m = \pi/\tau$ is to make the echo envelope decay faster than the spin-locked magnetization in a rotating rf field of amplitude $H_1 = \pi/4\gamma_I\tau$. Our experimental results in InP^{31} indicate, however, that the fast initial decay of the echo envelope [Fig. 5(b)] is not significantly different from the decay of the spin-locked magnetization in a rotating field of amplitude $H_1 = \pi/4\gamma_I\tau$. Thus the effect of the higher harmonics of the modulation only seems to affect the long time behavior of the echo envelope.

The result of our spin-locking experiments in InP^{31} can be understood if one assumes, for times $t \geq 0$ [Fig. 5(b)], a density matrix (in the rotating frame in the high-temperature approximation) of the form

$$\rho_e \simeq \frac{1}{\mathrm{Tr}(1)} + \frac{\hbar\gamma_I H_1 I_Z - \hbar\mathcal{H}^*_{IS}}{\mathrm{Tr}(1)k\theta_1} - \frac{\hbar\mathcal{H}_S}{\mathrm{Tr}(1)k\theta_2} \,, \qquad (22)$$

where the spin temperatures $\theta_1(t)$ and $\theta_2(t)$ determine the time dependence of $\rho_e(t)$.

The term

$$\mathcal{H}^*_{II} = \sum_{k>j} (A^I_{jk} \vec{I}_j \cdot \vec{I}_k + B^I_{jk} I_{jX} I_{kX})$$

in Eq. (21), representing spin-spin interactions between P^{31} nuclei, has been neglected in Eq. (22) compared to

$$\mathcal{H}^*_{IS} = \sum_{jk'} C^{IS}_{jk'} I_{jX} S_{k'z} \,.$$

The ratio of the heat capacities at common spin temperatures for the two terms is of the order $(\Delta H^2_{II})^{P^{31}}/3(\Delta H^2_{IS})^{P^{31}} \simeq 0.03$. Thus only a negligible fraction of the total energy will be involved in connection with $\mathcal{H}^*_{II}$.

The term $\mathcal{H}^*_{IS}$ in Eq. (22), which is non-negligible compared with the Zeeman term, is made time dependent by the flip-flop transitions of the nonresonant indium spins. For the values of H_1 in our experiments, this term can induce transitions between the Zeeman levels in the rotating frame.[31] Thus, the term $\mathcal{H}^*_{IS}$ establishes a thermal contact between the Zeeman-energy reservoir of the resonant spin and the nonresonant spin-energy reservoir associated with the term $\mathcal{H}_S$ in Eq. (20). The amount of effective energy exchanged between the two reservoirs until a uniform spin temperature in the rotating frame is achieved will depend on the spin-heat capacity of the reservoirs.

The density matrix [Eq. (22)] can be used together with Eq. (21) to calculate the effective energy[11] $E = \mathrm{Tr}(\hbar\mathcal{H}_{e\rho}\rho_e)$. The result is

$$E = -\frac{N\gamma_I^2\hbar^2 I(I+1)}{3k}\left(\frac{h_1^2 + H_1^2}{\theta_I} + \frac{h_2^2}{\theta_2}\right) , \qquad (23)$$

where $N = N_I = N_S$ is the total number of spins of each species. The parameters

$$h_1^2 = \mathrm{Tr}(\mathcal{H}^*_{IS})^2/\mathrm{Tr}(\gamma_I^2 I_Z^2)^2$$

and

$$h_2^2 = \mathrm{Tr}(\mathcal{H}_S)^2/\mathrm{Tr}(\gamma_I^2 I_Z^2)$$

determine the thermodynamic properties of the system. A value for $h_1^2 = (\Delta H^2_{IS})^{P^{31}} = 2.0\ G^2$, that includes the effect of the pseudodipolar interaction,

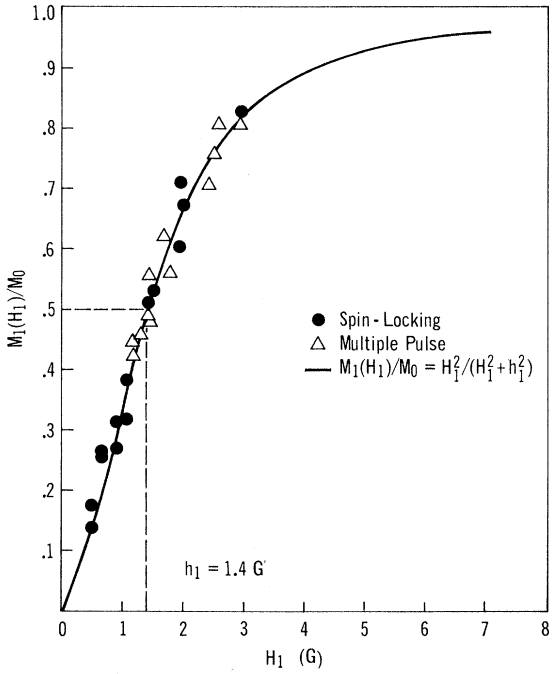

FIG. 6. P^{31} spin-locked magnetization as a function of effective field for a 500-μsec spin-locking rf pulse (•). The data obtained from the analogous multiple pulse experiments are indicated by △. The solid line is a plot of Eq. (26).

was obtained in Sec. II C. Although h_2^2 could also be determined from second-moment measurements on the indium resonance, the contribution to the second moment from the wings of the quadrupole broadened $In^{115,113}$ resonance in our samples was difficult to estimate. A value of h_2^2 considerably larger than the dipolar one,

$$[\gamma_S^2 S(S+1)\,(\Delta H_{SS}^2)_{\text{dipolar}}^{\text{In}^{115}}/3\gamma_I^2 I(I+1)] = 5.15\ \text{G}^2\,,$$

is expected.

Immediately after the 90° pulse in a spin-locking experiment at exact resonance, the effective energy has a value $E_i = -M_0H_1 - C(h_1^2+h_2^2)/\theta_0$, where $C = N\gamma_I^2\hbar^2 I(I+1)/3k$, θ_0 is the lattice temperature, and $M_0 = CH_0/\theta_0$ is the equilibrium magnetization. For $t=0$ [Fig. 5(b)], the effective energy is given by Eq. (23) and conservation of energy[38] implies

$$-M_0H_1 - \frac{C(h_1^2+h_2^2)}{\theta_0} = \frac{-C(h_1^2+H_1^2)}{\theta_1} - \frac{Ch_2^2}{\theta_2}\,. \tag{24}$$

If one assumes that the spin temperature in the rotating frame of the nonresonant spin reservoir is initially much higher than $\theta_1(t=0)$ and of the order of θ_0, one obtains for the ratio $M_1(H_1)/M_0 = H_1\theta_0/H_0\theta_1$:

$$M_1(H_1)/M_0 = H_1^2/(H_1^2+h_1^2)\,. \tag{25}$$

A plot of experimental values $M_1(H_1)/M_0$ as a function of H_1 in InP^{31} is shown in Fig. 6. The data were obtained using sample 7 from spin-locking and multiple-pulse experiments, and in both cases the point $t=0$ [Fig. 5(b)] was chosen at $t'=500$ μsec. Also shown in Fig. 6 is a plot of $M_1(H_1)/M_0$ as given by Eq. (25) with $h_1^2 = 1.97$ G^2. A good agreement between h_1^2 and $(\Delta H_{IS}^2)^{P^{31}}$ is obtained independently of sample material.

Unlike the case discussed by McArthur, Hahn, and Walstedt,[14] the coupling term $\mathcal{H}_{IS}^*$ in Eq. (22) is non-negligible. The assignment of a common spin temperature to it and the Zeeman term is in agreement with our experimental results.

B. Cross Relaxation in Rotating Frame

The assumption can be made[14,41] that $\theta_1^{-1}(t)$ and $\theta_2^{-1}(t)$ relax toward a common spin temperature in a way described by the simple rate equation

$$\frac{d\theta_1^{-1}}{dt} = -T_\epsilon^{-1}(\theta_1^{-1} - \theta_2^{-1})\,. \tag{26}$$

Since the effective energy is conserved between the two reservoirs characterized by $E_1(\theta_1) = -C(h_1^2+H_1^2)/\theta_1$ and $E_2(\theta_2) = -Ch_2^2/\theta_2$, one has, in addition to (26), $d(E_1+E_2)/dt = 0$. A solution for $M_z(t) = CH_1\theta_1^{-1}(t)$ is easily found if the initial conditions $\theta_1^{-1}(0) = \theta_0^{-1}H_0H_1/(H_1^2+h_1^2)$ and $\theta_2^{-1}(0) \simeq \theta_0^{-1} \ll \theta_1^{-1}$ are included:

$$\frac{M_z(t)}{M_0} = \frac{H_1^2}{h_1^2+H_1^2}\left\{\frac{h_1^2+H_1^2}{h_1^2+h_2^2+H_1^2} + \frac{h_2^2}{h_1^2+h_2^2+H_1^2}\exp\left[-\frac{t}{T_\epsilon}\left(1+\frac{h_1^2+H_1^2}{h_2^2}\right)\right]\right\}. \tag{27}$$

A plot of experimental values $M_z(t)/M_0$ as a function of time measured from $t=0$ [Fig. 5(b)] is shown in Fig. 7. Also shown is a plot of $M_z(t)/M_0$ given by Eq. (27), where h_2^2 and T_ϵ are adjustable parameters. The multiple-pulse data in Fig. 7 were obtained by subtracting from the echo envelope the slow final exponential decay and adding the constant value $M_2(H_1)$ [Fig. 5(b)]. The agreement with the spin-locking data, that is plotted directly in Fig. 7 for a typical effective field $H_1 = 1.25$ G, is satisfactory.

A value $h_2^2 = 35 \pm 5$ G^2 is obtained from the experimental data on sample 7. The large value of h_2^2 has some implications. The ratio $M_z(0)/M_z(\infty)$ that determines the magnitude of the cross-relaxation effect can be expressed in terms of the heat

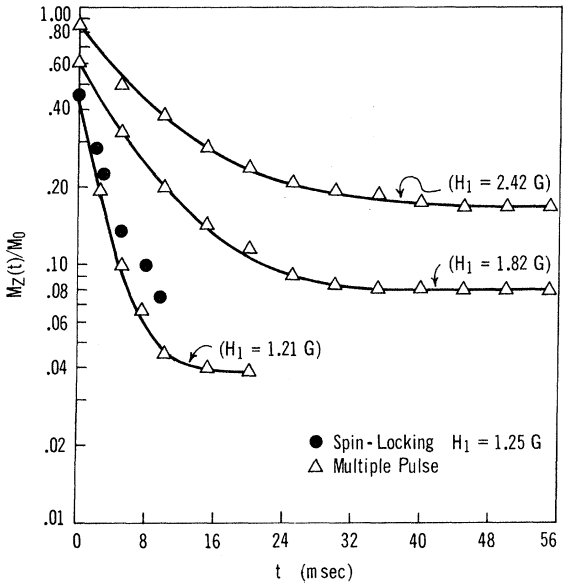

FIG. 7. Time evolution of the rotating frame magnetization in sample 7 as a function of effective field H_1: from multiple-pulse experiments as described in the text (△) and from spin-locking experiments (●). The solid lines are the time evolutions predicted by Eq. (27).

capacities $\mathcal{C}_1 = \partial E_1(\theta_1)/\partial\theta_1$ and $\mathcal{C}_2 = \partial E_2(\theta_2)/\partial\theta_2$ of the reservoirs. From Eq. (27) one obtains

$$M_Z(0)/M_Z(\infty) = (h_1^2 + H_1^2 + h_2^2)/(h_1^2 + H_1^2) = 1 + \mathcal{C}_2(\theta_f)/\mathcal{C}_1(\theta_f) . \quad (28)$$

It is clear from Eq. (28) that a necessary condition for the observability of the cross-relaxation effect described here is that the heat capacity $\mathcal{C}_1$ of the initially colder reservoir be small enough compared with $\mathcal{C}_2$ for the range of values of H_1 of interest. Since in our case $(h_2^2/h_1^2) = 17$, this condition is well satisfied. It is interesting to notice, however, that for $Na^{23}F$ with the magnetic field along the [100] direction,[39] one has instead $(h_2^2/h_1^2) = 0.17$. Thus, $M_Z(0) \simeq M_Z(\infty)$ for all values of H_1, and the cross-relaxation effect would be negligible.

From Eq. (27) one obtains $T_\epsilon = T_{IS}[1 + (h_1^2 + H_1^2)/h_2^2]$, which gives the cross-relaxation time T_ϵ in terms of the time constant T_{IS}. McArthur, Hahn, and Walstedt[14] calculated the cross-relaxation rate produced by the coupling Hamiltonian $\mathcal{H}_{IS}^*$ considered as a small perturbation. They obtained excellent agreement with their experimental data on the Ca^{43}-F^{19} spin system by assuming a Lorentzian autocorrelation function for the operator $\sum_{k'} C_{jk'}^{IS} S_{k'z}$. Several factors make such a calculation much more complicated in the case of InP. The coupling Hamiltonian is not negligibly small compared to the other terms in Eq. (21). In addition, the contributions to $\mathcal{H}_S = \mathcal{H}_{SS} + \mathcal{H}_Q^S$ from electron-coupled interactions and electric-quadrupole interactions are not known.

Figure 8 shows a semilogarithmic plot of T_ϵ as a function of H_1. The data were obtained from multiple pulse experiments on sample 6. One can compare with the expression obtained in Ref. 14:

$$T_\epsilon^{-1} = \tfrac{1}{2}\pi(\Delta\omega_{IS}^2)^{P^{31}} \tau_c e^{-\gamma_I H_1 \tau_c} . \quad (29)$$

The data on sample 6 do not deviate considerably from an exponential dependence on H_1. From the slope of the straight line, a correlation time $\tau_c = 64$ μsec is obtained. The values of T_ϵ calculated from Eq. (29) are, however, smaller than the experimental ones by about a factor of 40. The reason for the large discrepancy is not well understood. A possible explanation is that flip-flop transitions between In^{115} levels other than $m = \pm\frac{1}{2}$ are strongly inhibited. Because of first-order quadrupole broadening, transitions involving these levels may occur at a rate too slow to produce cross relaxation of the P^{31} Zeeman levels in the rotating frame. The appropriate spectral density would then be that corresponding to an effective spin $S^* = \frac{1}{2}$, and the values of T_ϵ would be increased from Eq. (29) by a factor

$$\mathrm{Tr}(S_{k'z})^2/\mathrm{Tr}(S_{k'z}^*)^2 = S(S+1)/S^*(S^*+1) = 33 .$$

Although the doped InP samples exhibit longer values of T_ϵ as expected, additional experiments with single crystals free of impurities or imperfactions would be required to test our assumptions.

The value of the correlation time τ_c obtained from the slope of the straight line in Fig. 8 is much

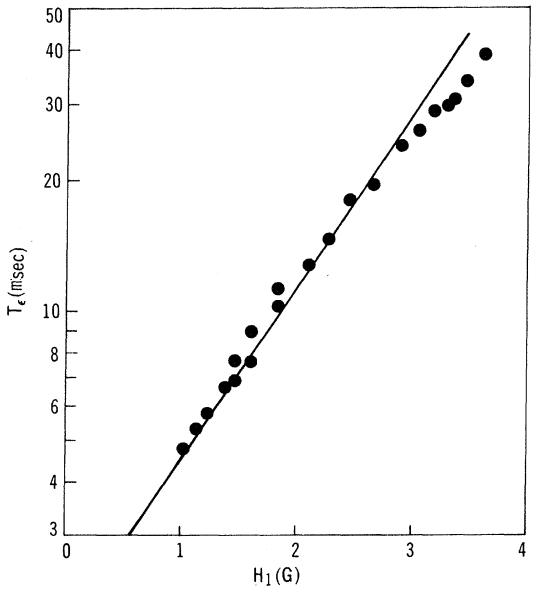

FIG. 8. Cross-relaxation time T_ϵ as a function of effective field in sample 6.

smaller than the cross-relaxation time T_ϵ for the range of values of H_1 in our experiments. It should be pointed out that a simple exponential energy-transfer process can only be observed if the cross-relaxation time T_ϵ is long enough. Otherwise, the initial oscillatory behavior [Fig. 5(a)] would coalesce with the process described by the time constant T_{IS}, and Eq. (26) would no longer describe the experimental conditions.

IV. SUMMARY

It has proved possible, through measurements made on "solid echoes," to separate some contributions to the second moment of the InP^{31} resonance. The contribution from $P^{31}-P^{31}$ interactions agrees with the dipolar value. The dominant $P^{31}-In^{115,113}$ contribution, however, is about a factor of 2 smaller than the dipolar value. A proposed explanation of this result is based on the assumption that the P–In pseudodipolar interaction $\tilde{B}^{IS}_{jk'}$ in InP and the magnetic dipole-dipole interaction have the same order to magnitude but opposite sign. In addition, the indirect-exchange interaction $\tilde{A}^{IS}_{jk'}$ is smaller than $\tilde{B}^{IS}_{jk'}$. A ratio $|\tilde{B}^{IS}/\tilde{A}^{IS}| \simeq 1.8$ accounts for the experimentally observed second moments. The negative sign of $\tilde{B}^{IS}_{jk'}$ in InP is in agreement with the prediction of a simple localized-bond model proposed by Bloembergen and Sorokin.

A thermodynamical model has been used to interpret the evolution of the P^{31} magnetization along the effective field in the rotating frame. The observation of a significant cross-relaxation effect and its description by a simple rate equation were attributed to: (a) the large spin heat capacity of the nonresonant spin reservoir and (b) a cross-relaxation time which is much longer than the correlation time of the In–P coupling operator, randomly modulated by the flip-flop transitions between indium spins.

ACKNOWLEDGMENTS

The authors are indebted to Professor R. K. Sundfors, who made available the spectrometer used to obtain the cw data, for his interest and assistance, and for many stimulating discussions. We also wish to express our gratitude to Professor K. Luszczynski and Dr. J. G. Broerman for many helpful suggestions. The indium phosphide samples used in this investigation were obtained through the courtesy of the New Enterprise Division of the Monsanto Co.

---

†Work supported in part by the U. S. Air Force Office of Scientific Research.

*Present address: Department of Physics, University of Pittsburgh, Pittsburgh, Pa.

[1]R. L. Mieher, in *Semiconductors and Semimetals*, edited by R. K. Willardson and A. G. Beer (Academic, New York, 1966), Vol. II, Chap. 7.

[2]M. A. Ruderman and C. Kittel, Phys. Rev. 96, 99 (1954).

[3]N. Bloembergen and T. J. Rowland, Phys. Rev. 97, 1679 (1955).

[4]P. W. Anderson, Phys. Rev. 99, 623 (1955).

[5]R. G. Shulman, J. M. Mays, and D. W. McCall, Phys. Rev. 100, 692 (1955).

[6]R. G. Shulman, B. J. Wyluda, and H. R. Hrostowsky, Phys. Rev. 109, 808 (1958).

[7]M. J. Weber, J. Phys. Chem. Solids 21, 210 (1961).

[8]R. K. Sundfors, Phys. Rev. 185, 458 (1969).

[9]A. N. Gusatinskii and S. A. Nemnonov, in *Collection: Thermodynamics and Chemical Binding in Semiconductors*, edited by N. N. Sirota (Consultants Bureau, New York, 1968).

[10]A. G. Redfield, Phys. Rev. 98, 1787 (1955).

[11]L. C. Hebel, Solid State Phys. 15, 409 (1963).

[12]M. Goldman, *Spin Temperature and Nuclear Magnetic Resonance in Solids* (Oxford U. P., New York, 1970).

[13]F. M. Lurie and C. P. Slichter, Phys. Rev. 133, A1108 (1964).

[14]D. A. McArthur, E. L. Hahn, and R. E. Walstedt, Phys. Rev. 188, 609 (1969).

[15]G. D. Watkins, Ph. D. thesis (Harvard University, 1952) (unpublished).

[16]I. J. Lowe and R. E. Norberg, Phys. Rev. 107, 46 (1957).

[17]J. G. Powles and H. G. Strange, Proc. Phys. Soc. (London) 82, 6 (1963).

[18]E. R. Andrew, Phys. Rev. 91, 425 (1953).

[19]H. Lütgemeier, Z. Naturforsch. 192, 1297 (1964).

[20]G. E. Pake and E. M. Purcell, Phys. Rev. 74, 1184 (1948).

[21]P. Mansfield, Phys. Rev. 137, A961 (1965).

[22]M. E. Emshwiller, E. L. Hahn, and D. Kaplan, Phys. Rev. 118, 414 (1960).

[23]W. W. Warren, Jr. and R. E. Norberg, Phys. Rev. 154, 277 (1967).

[24]J. H. Van Vleck, Phys. Rev. 74, 1168 (1948).

[25]H. S. Gutowsky and B. R. McGarvey, J. Chem. Phys. 20, 1472 (1952).

[26]G. Giesecke and H. Pfister, Acta Cryst. 11, 369 (1958).

[27]B. Goldstein, Phys. Rev. 121, 1305 (1961).

[28]E. H. Rhoderick, J. Phys. Chem. Solids 8, 498 (1959).

[29]A. Abragam and J. Winter, Compt. Rend. 249, 1633 (1959).

[30]M. Engelsberg and R. E. Norberg, Phys. Letters 31A, 311 (1970).

[31]N. Bloembergen and P. P. Sorokin, Phys. Rev. 110, 865 (1958).

[32]S. Clough and W. I. Goldburg, J. Chem. Phys. 45, 4080 (1966).

[33]K. Yosida and T. Moriya, J. Phys. Soc. Japan 11, 33 (1956).

[34]F. H. Pollak, C. W. Higginbotham, and M. Cardona, J. Phys. Soc. Japan Suppl. 21, 20 (1966).

[35]M. Cardona, in *Semiconductors and Semimetals*, edited by R. K. Willardson and A. G. Beer (Academic, New York, 1966), Vol. III, Chap. 5.

[36]D. C. Look and I. J. Lowe, J. Chem. Phys. 44, 2995

(1966).
[37]J. S. Waugh and C. H. Wang, Phys. Rev. 162, 209 (1967).
[38]P. Mansfield and D. Ware, Phys. Rev. 168, 318 (1968).
[39]P. Mansfield, K. H. B. Richards, and D. Ware, Phys. Rev. B 1, 2048 (1970).
[40]R. L. Mieher, Phys. Rev. 125, 1537 (1962).
[41]R. E. Walstedt, Phys. Rev. 138, A1096 (1965).

PHYSICAL REVIEW B VOLUME 5, NUMBER 9 1 MAY 1972

Nuclear-Magnetic-Resonance Measurement of the Conduction-Electron g Factor in CdTe†

D. C. Look
Department of Physics, University of Dayton, Dayton, Ohio 45409

and

D. L. Moore
Air Force Institute of Technology, Wright-Patterson Air Force Base, Dayton, Ohio 45433
(Received 26 April 1971)

The effective g factor g^* of conduction electrons in degenerate CdTe has been determined by using measurements of the Cd^{113} nuclear spin-lattice relaxation time T_1 and the Knight shift K. It is shown that the magnitude of g^* is given by the Korringa product $T_1TK^2 = C(g^*)^2$, where C is a known constant and T is the absolute temperature, and that the sign of g^* is given by the sign of K for a spherically symmetric conduction band. The measured value, $g^* = -1.1 \pm 0.1$, is within the range allowed by effective-mass theory. Also, the electronic probability density at the nucleus, normalized to unity in an atomic volume, is calculated to be $|\psi_F(0)|^2 \simeq 6.5 \times 10^{25}$ cm^{-3}, about 70% of that found for the free Cd ion in a $5s\,^2S_{1/2}$ state.

I. INTRODUCTION

For many semiconductors it is found that the magnetic spin splitting of conduction electrons is given by an effective g factor g^*, which is different from two, the free-electron value.[1] This effect has been successfully explained, using the effective-mass formalism,[2] as being due to a nearby band which is connected to the conduction band by momentum matrix elements and which is split by spin-orbit interaction.[3] In cases where the band gap is small and the spin-orbit energy large, the g factor can be greatly affected; for example, in InSb it is found[3] that $g^* \simeq -50$.

In the II–VI compound sequence, CdS, CdSe, and CdTe, the band gaps decrease and the spin-orbit energies increase.[4] The g factors are expected to decrease in this sequence, and indeed they do for the first two, which have been measured by electron-paramagnetic-resonance (EPR) and magneto-optical methods to be $g^*_{CdS} \simeq 1.72$–1.79 and $g^*_{CdSe} \simeq 0.51$–0.7. For CdTe Cardona[4] has calculated $g^*_{CdTe} \simeq -0.4$. Evidently, attempts to measure g^*_{CdTe} by EPR have proved unsuccessful.[5]

It is often true that conduction electrons have s-state character and thus interact with magnetic nuclei through the hyperfine-contact coupling.[6] Because the electron spins are polarized in a magnetic field, the diagonal part of the hyperfine Hamiltonian produces a shift in the nuclear-magnetic-resonance (NMR) frequency, the so-called Knight shift.[6] Since the degree of polarization depends upon g^*, we would expect to gain information through measurement of this shift. Furthermore, the fluctuating off-diagonal elements of the Hamiltonian produce a nuclear-spin-lattice relaxation mechanism,[6] and measurements of the relaxation time, in conjunction with the Knight shift, afford a means of eliminating all unknown parameters except g^*. Our result for g^* in CdTe, although somewhat different from Cardona's estimate,[4] is not outside the range allowed by his calculation, considering the spread in measured and estimated energy-band parameters.

II. THEORY

A. Effective-Mass Theory

It is well known that the effect of a magnetic field on Bloch functions is quite appreciable and cannot adequately be treated by perturbation theory.[1] However, because the electrons of interest in a semiconductor often occupy only a small region of k space, it is possible to obtain an approximation to the Hamiltonian by carrying out a perturbation expansion in powers of the wave vector[2]; to lowest order, this is the so-called effective-mass Hamiltonian. Furthermore, since the energy levels still remain clustered in bands, and *interband* matrix elements are usually quite small, the Ham-

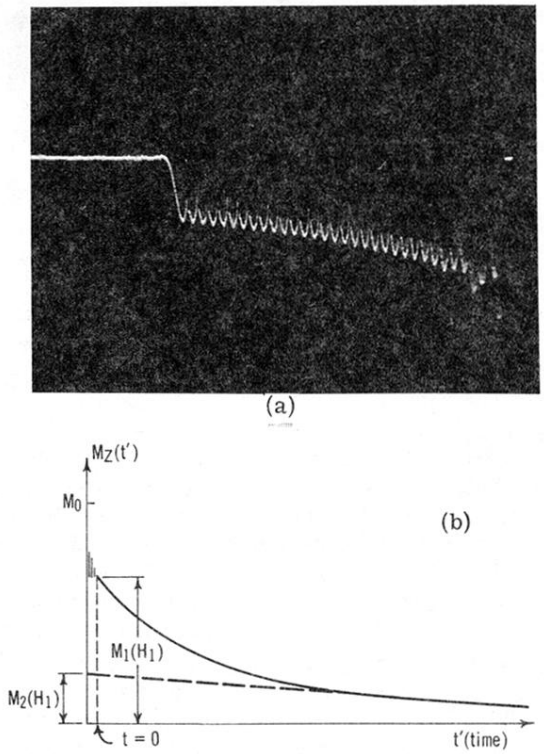

FIG. 5. (a) Oscilloscope photograph of a train of "solid echoes" for a $90°\text{-}\tau\text{-}90°_{90°}\text{-}2\tau\text{-}90°_{90°}\text{-}2\tau\text{-}90°_{90°}\text{-}\cdots$ pulse sequence in InP^{31}. The pulse separation is $2\tau = 100$ μsec and the sweep is 0.5 msec/large div. (b) Sketch of the echo envelope showing the fast initial decay and the slower final decay. The total time is typically 20 times longer than in (a).